Korean J. Chem. Eng., 32(2), 222-229 (2015)
DOI: 10.1007/s11814-014-0224-y

pISSN: 0256-1115
eISSN: 1975-7220

Interfacial resistance in CO_2-normal alkane and N_2-normal alkane systems: An experimental and modeling investigation

Fatemeh Nikkhou*, Peyman Keshavarz*,†, Shahab Ayatollahi, and Ali Zolghadr****

*School of Chemical and Petroleum Engineering, Chemical Engineering Department, Shiraz University, Shiraz, Iran
**Enhanced Oil Recovery Research Centre, School of Chemical and Petroleum Engineering, Shiraz University, Shiraz, Iran
(*Received 25 May 2014 • accepted 4 August 2014*)

Abstract−Gas-liquid systems are one of the most common systems which appear in hydrocarbon reservoirs; therefore, the investigation of the interfacial properties and effect of temperature and pressure on these systems is crucial for optimizing the plan of production. In this study, interfacial resistances for N_2-alkane and CO_2-alkane systems were estimated at different pressures and temperatures. A model was developed to calculate interfacial resistance using the equilibrium and dynamic interfacial tension data which were measured by pendant drop technique at different pressures and temperatures. Interfacial resistances were estimated for a temperature range from 313 to 393 K and pressures from 0.34 to 41.7 MPa. The results showed that interfacial resistance in N_2-alkane and CO_2-alkane systems decreased at higher pressure. Moreover, In N_2-alkane systems, the interfacial resistance decreases as the temperature increases; however, in CO_2-alkane system the interfacial resistance depends on the diffusion and solubility interactions; it will decrease, increase or remain constant.

Keywords: Interfacial Resistance, Interfacial Tension, Carbon Dioxide, Nitrogen, Normal Alkanes

INTRODUCTION

When gas and liquid phases are in contact, molecules diffuse from one phase to another, which leads to some changes in interfacial properties of the system [1,2]. These properties are mostly described using the dynamic interfacial tension (IFT) and interfacial mass transfer resistance [3-5]. The IFT as the interface property is believed to have the most vital role in the mass transfer process between the two phases [6,7].

There are three different resistances involved in the mass transfer between the two phases in gas-liquid systems: gas bulk, interface, and liquid bulk resistances. In some cases, interface acts as a resistive layer and hinders the molecular diffusion. Some previous studies have ignored this resistance and only considered bulk resistances [8-12]. They argued that in practical situations, this parameter is not significant [13-15] or it becomes influential in the conditions where insoluble substances spread over the liquid surface and postpone the mass transfer process [16].

For modeling a mass transfer process in the presence of interfacial resistance, diffusion equation is applied to the interface and a non-equilibrium boundary condition is introduced to the model. Then the model is solved and interfacial resistance is evaluated through the interface. Reamer et al. [17] developed a model for the methane-oil system by assuming an interfacial resistance and a non-equilibrium boundary condition between phases. Walas [18] also solved this mass transfer model analytically, in the form of infinite Fourier series. The non-equilibrium boundary condition becomes important when the gas and liquid phases are brought into contact at high pressures, in which there is not enough time for the phases to reach the equilibrium conditions [19].

Mass transfer also can be modeled by examining three different boundary conditions (equilibrium, quasi-equilibrium and non-equilibrium) using pressure decay method. In this technique, pressure in the gas phase decreases continuously as a result of diffusion. Results showed that a non-equilibrium boundary condition is more appropriate compared to the equilibrium and quasi-equilibrium boundary conditions for CO_2-heavy oil system [20]. On the other hand, Saboorian's [21] results showed that the non-equilibrium boundary condition does not affect the gas diffusion process significantly; however it is more realistic physically. Most of the previous studies [22-26] have been conducted utilizing pressure decay method for calculating diffusion coefficient and interface mass transfer coefficient. Although this technique requires a simple experimental setup, it is time-consuming, and since pressure reduces monotonically during the process, the effect of pressure on diffusion coefficient cannot be determined [27,28].

A novel experimental technique was introduced by Yang and Gu for estimating interfacial resistance in gas-liquid systems. In this method the diffusivity and interface mass transfer coefficient are estimated using dynamic and equilibrium IFT data [1,2]. They conducted their tests using pendant drop method as a remarkably fast and inexpensive technique [29,30]. This method requires smaller volume of fluid compared to other methods [1]. Mass transfer parameters are obtained as a result of dynamic IFT reduction. This method assumes a non-equilibrium boundary condition, which allows calculation of interfacial resistance. In previous studies, interfacial resistance has been evaluated at constant temperature and limited range of pressures and for specific systems [2,19].

†To whom correspondence should be addressed.
E-mail: pkeshavarz@shirazu.ac.ir

In this study, interfacial resistance of N_2-liquid hydrocarbon systems was measured and compared with those of CO_2-liquid hydrocarbon mixtures. Hexadecane and heptane were chosen as the representative of liquid components of oil. Mass transfer model implemented in these systems includes a non-equilibrium boundary condition in order to examine resistance in the interface and be in acceptable agreement with experimental data. In addition, the effects of pressure (0.34 to 41.7) MPa and temperature (313.15 to 393.15) K on the interfacial resistance of studied systems were investigated and the role of diffusion and solubility in those systems were illustrated.

EXPERIMENTAL SECTION

1. Materials

CO_2 and N_2 used for the experiments were provided from Pars Balloon Co., Iran. Heptane and hexadecane were supplied by Merck, Co., Germany. The purities of applied nitrogen, carbon dioxide, heptane and hexadecane were 99.9%, 99.5%, >99.0%, >99.0%, respectively.

2. Experimental Apparatus and Procedure

The dynamic and equilibrium interfacial tensions of CO_2/liquid hydrocarbon and N_2/liquid hydrocarbon systems at extensive ranges of temperatures and pressures were measured with the apparatus IFT700 (Vinci Technologies). Fig. 1 shows the schematic of IFT measurements setup. A high pressure cell with a volume of 20 cm^3 allows IFT measurements at different pressures and temperatures. The experimental setup has been described in details, elsewhere [31].

Initially, the entire system (capillary injector, line connections, bulk cylinder, drop and view chamber) was washed with toluene and acetone followed by deionized water, and finally flushed by purging high grade nitrogen. Then nitrogen/carbon dioxide was introduced to the bulk tank using a syringe pump at specified pressure and liquid was transferred to the drop tank. The heater was set at the required temperature. After reaching the equilibrium condition, the high pressure cell was pressurized with bulk fluid to the specified pressure and a liquid drop was introduced to the chamber from the drop cylinder. After formation of a well-formed drop at the tip of the needle, sequential digital images were taken by camera and analyzed utilizing drop analysis system software of the rig to evaluate dynamic and equilibrium interfacial tensions of the pendant drop. The pendant drop tests were repeated for at least three times to ensure satisfactory repeatability for each pressure and temperature. The standard uncertainty calculations are explained in detail, elsewhere [31].

MODELING

1. Mass Transfer Model

Fig. 2 schematically illustrates a well-shaped pendant drop surrounded by high pressure nitrogen gas. Inner radius and height of the needle are expressed by r_n and h_n, respectively. φ is the physical domain which has been occupied by liquid phase, B_{im} is boundaries formed between liquid phase and impermeable surfaces like the needle's wall, and B_{int} is boundary between gas and liquid phases.

The diffusion process results in IFT reduction, extraction of light components of heavy phase, and oil-swelling [3,4,33]. These phenomena affect the mass transfer process and make it more complicated [1]. However, due to problems associated with the numerical simulation of the systems under study, the following assumptions have been made:

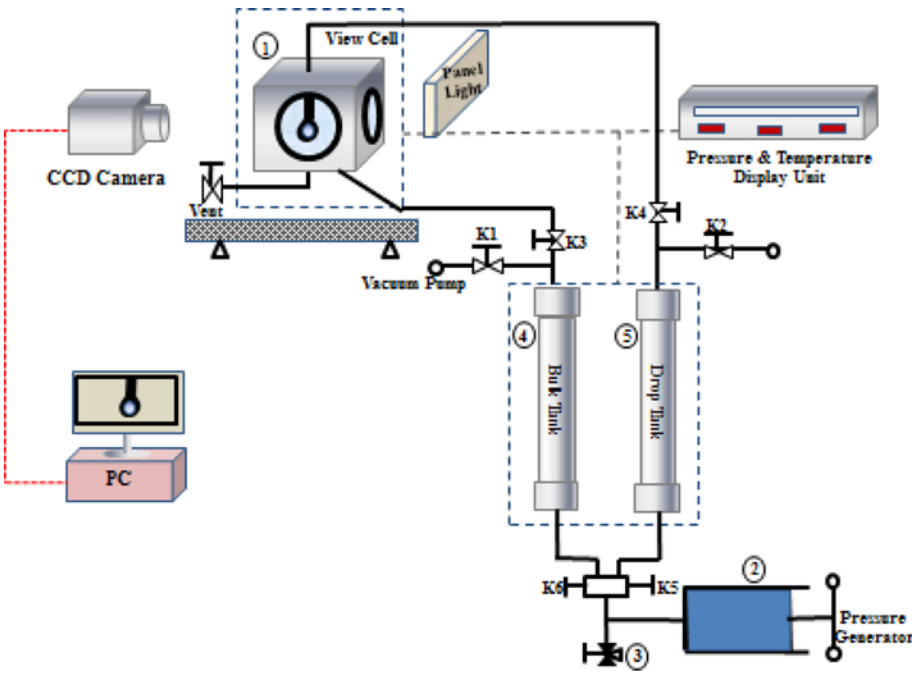

Fig. 1. Schematic of the experimental setup used for IFT measurement.
① View cell ② Pressure generator ③ Pressure manometer ④ Bulk tank ⑤ Drop tank [31,32]

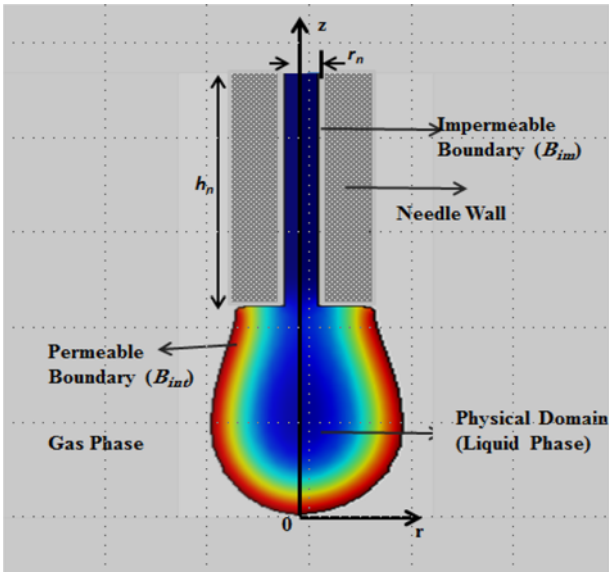

Fig. 2. A dynamic pendant hydrocarbon drop which is surrounded by high pressure gas.

1. All systems are assumed to be binary.
2. No chemical reaction occurs during diffusion process.
3. Pressure and temperature remain constant during the experiment. In the modeling, the surrounding gas phase is very large in comparison with the liquid drop phase in terms of their volumetric ratio. Meanwhile, GOR, a petroleum terminology, is defined as the gas-oil ratio in volume at the actual pressure and temperature is equal to 4,000 : 1 in the experimental conditions. Therefore, the pressure reduction in the gas phase is negligible.
4. Swelling effect is assumed to be negligible because the diffusion process is very slow.

Interfacial resistance is not negligible in comparison with gas and liquid bulk resistances [20]. Therefore, in this study a non-equilibrium boundary condition is applied to the model in order to evaluate the interfacial resistance. In this case, governing mass transfer equation can be expressed as [34]:

$$\frac{\partial c}{\partial t}=D\left[\frac{1}{r}\frac{\partial}{\partial r}\left(r\frac{\partial c}{\partial r}\right)+\frac{\partial^2 c}{\partial z^2}\right],\ (r,z)\in\varphi,\ t>0 \tag{1}$$

where c is gas concentration in the liquid phase, t is time, and D is diffusion coefficient. φ is the physical domain for diffusion process and r and z are the radial and axial coordinates, respectively. Initially, no gas has been dissolved in the liquid phase; therefore initial condition for this problem is considered as follows:

$$c(r,z,t)=0,\ (r,z)\in\varphi,\ t=0 \tag{2}$$

Because gas molecules cannot diffuse through the needle's wall, molar flux equals zero and the first boundary condition is:

$$D\left(\frac{\partial c}{\partial r}n_r+\frac{\partial c}{\partial z}n_z\right)=0,\ (r,z)\in B_{im} \tag{3}$$

In this formula n_r and n_z are the direction cosines. The second boundary condition is a non-equilibrium Robin type boundary condition which the diffusion process is modeled in the presence of interfacial resistance. This boundary condition is expressed as [19,35]:

$$D\left(\frac{\partial c}{\partial r}n_r+\frac{\partial c}{\partial z}n_z\right)=k(c_{eq}-c(r,z,t)),\ (r,z)\in B_{int} \tag{4}$$

where k is the interface mass transfer coefficient and C_{eq} is the equilibrium concentration of gas in liquid phase. The above-mentioned equations can be expressed in dimensionless form using the following dimensionless variables:

$$C=\frac{c}{c_{eq}},\ R=\frac{r}{r_n},\ Z=\frac{z}{r_n},\ \tau=\frac{Dt}{r_n^2},\ k_D=\frac{kr_n}{D} \tag{5}$$

where C is the dimensionless gas concentration in the liquid phase, R and Z are dimensionless radial and axial coordinates, respectively; τ is the dimensionless time, and k_D is the mass transfer Biot number. k_D indicates the ratio of the bulk resistance (r_n/D) to the interfacial resistance (1/k). Low values of k_D, represents significant amount of interfacial resistance [19,22,36]. Dimensionless forms of Eqs. (1) to (4) are:

$$\frac{\partial C}{\partial \tau}=\frac{1}{R}\frac{\partial}{\partial R}\left(R\frac{\partial C}{\partial R}\right)+\frac{\partial^2 C}{\partial Z^2},\ (R,Z)\in\theta,\ \tau>0 \tag{6}$$

$$C(R,Z,\tau)=0,\ (R,Z)\in\theta,\ \tau=0 \tag{7}$$

$$\left(\frac{\partial C}{\partial R}n_R+\frac{\partial C}{\partial Z}n_Z\right)=0(R,Z)\in B_{im} \tag{8}$$

$$\left(\frac{\partial C}{\partial R}n_R+\frac{\partial C}{\partial Z}n_Z\right)=k_D[1-C(R,Z,\tau)],\ (R,Z)\in B_{int} \tag{9}$$

where θ is the computational domain.

2. Numerical Method

To evaluate the interfacial resistance, first the interface mass transfer coefficient was calculated using mass transfer equations (Eqs. (6) to (9)). For this purpose, the following procedure was followed:

1. Dynamic IFT data were recorded at specific pressure and temperature as a function of time. Equilibrium IFT data versus pressure [32] were measured and then converted into the equilibrium IFT data versus equilibrium gas concentrations which are nominated as calibration curves.
2. A diffusion coefficient was introduced to Eqs. (6) to (9) using available experimental data [37,38].
3. An initial value was assumed for interface mass transfer coefficient.
4. To solve the model, central finite difference method was applied to evaluate the dimensionless gas concentration profile using MATLAB programming software. The partial differential equation was discretized implicitly, which generated sets of simultaneous algebraic equations. Gauss-Seidel iteration was used to solve this system of algebraic equations.
5. Using calibration curves of the measured IFT, the dynamic IFT at any time (t) was estimated by using the linear interpolation of the calibration curve, for assumed interface mass transfer coefficient.
6. Measured and estimated dynamic Interfacial tensions were compared. If their difference was less than an acceptable error, ε, then, the suggested interface mass transfer coefficient would be acceptable; otherwise, the initial assumption was changed and steps 3 through 6 were repeated. This difference was quantified by defin-

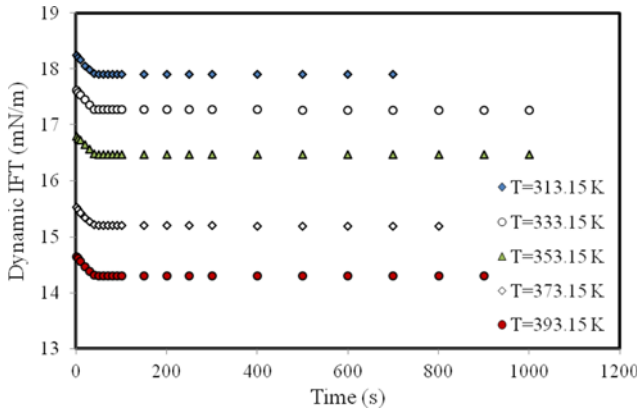

Fig. 3. Experimental measurement of dynamic IFT for N_2/ hexadecane system at 3.1 MPa and different temperatures.

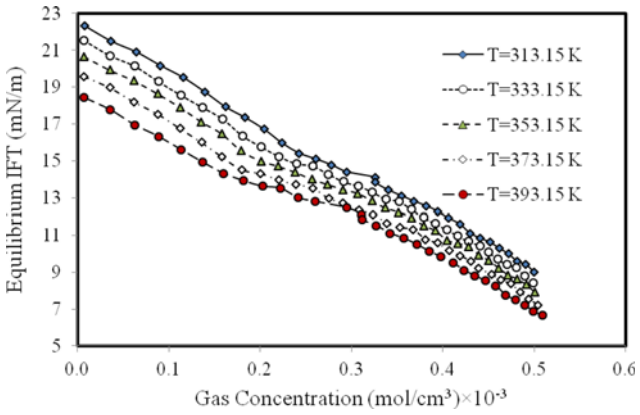

Fig. 5. Calibration curves for N_2/hexadecane mixture at temperature range of 313.15 to 393.15 K.

ing an objective function in Eq. (10).

$$E = \sqrt{\frac{1}{N}\sum_{i=1}^{N}\left[\frac{IFT_{exp}(t) - IFT_{cal}(t)}{IFT_{exp}(t)}\right]^2} \times 100\% \quad (10)$$

RESULTS AND DISSCUSION

1. Dynamic and Equilibrium IFT Measurement

Interactions between two immiscible phases, gas and oil in this case, result in the changes of IFT with time, known as dynamic interfacial tension. Fig. 3 shows dynamic IFT changes for N_2/hexadecane system at 3.1 MPa and for five different temperatures. Dynamic IFT data were measured using pendant drop method for a temperature range from 313 to 393 K and pressures from 0.34 to 41.7 MPa (For other systems see Fig. S1 of the Supplementary data).

The final value of dynamic IFT is referred to as equilibrium IFT [39]. Fig. 4 shows equilibrium IFT for N_2/hexadecane mixture at various pressures from 0.34 to 41.7 MPa and temperatures from 313 to 393 K [32].

According to the results shown in Fig. 4, equilibrium IFT declined as the pressure increased at each constant temperature. This reduction is due to improved gas solubility at higher pressures [40-43]. Equilibrium pressures can be converted to equilibrium gas concentration using either a correlation or an equation of state [44]. In this work, the Soave-Redlich-Kwong (SRK) equation of state was used to perform this conversion. The reasons for choosing this equation of state and details of mathematical procedure can be found elsewhere [41]. In Fig. 5 equilibrium IFT are plotted versus calculated gas concentration known as calibration curves [1,2]. In these curves, equilibrium IFT was reduced almost linearly as the gas concentration increased, which could be due to the effect of higher gas solubility.

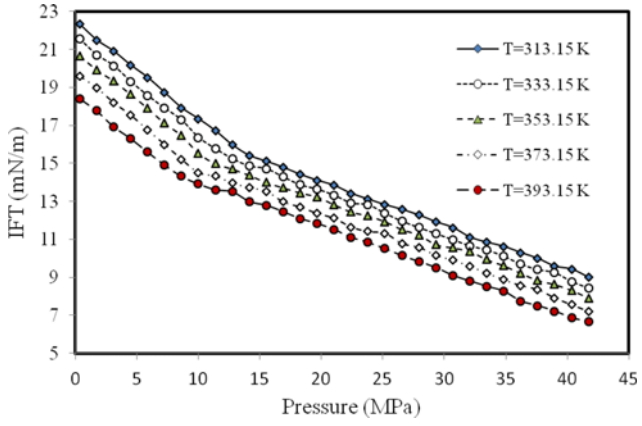

Fig. 4. Measured equilibrium interfacial tension versus pressure for N_2/hexadecane mixture [32].

2. Evaluation of Interface Mass Transfer Coefficient in N_2/Liquid Hydrocarbon Systems

To take into account a non-equilibrium boundary condition, interfacial resistance (1/k) was introduced to the mass transfer model via k_D in Eqs. (6) to (9). Interface mass transfer coefficient should be determined through the model initially to estimate interfacial resistance parameter. For this purpose, an initial value was assumed for interface mass transfer coefficient and Biot number was evaluated and used in Eq. (9). Then, gas concentration in the liquid phase is determined using SRK equation of state. In the next step, using calibration curves, dynamic IFT was calculated and compared with experimental dynamic IFT which was measured at specified temperature and pressure. If experimental and calculated dynamic IFT had small differences, estimated value for interface mass transfer coefficient would be accepted as the final value; otherwise, initial assumptions for this parameter should be corrected and above steps would be repeated. We studied ranges of pressure and temperature are 0.34 to 41.7 MPa and 313 to 393 K, respectively. Table 1 compares the results of interface mass transfer coefficient evaluated in this study with previous studies. It can be concluded that our results are in good agreement with other published data.

3. Investigating the Effects of Pressure and Temperature on Interfacial Resistance

Fig. 6 shows changes of interfacial resistance (1/k) versus temperature at different pressures for N_2/hexadecane system.

As Fig. 6 shows, interfacial resistance in N_2/hexadecane system decreases as the temperature increases. The reason is attributed to the enhancement of kinetic energy of gas molecules that leads to

Table 1. Comparison of calculated interface mass transfer coefficient at different temperatures and pressures

System Type	Pressure/MPa	Temperature/K	$D/10^{-9}$ m^2/s	$k/10^{-5}$ m/s	k_D	References
Model (CO_2/heptane)	1.72-4.48	313.15-393.15	8.28-17.88	6-120	0.56-108.6	This work
Model (CO_2/hexadecane)	1.72-8.6	313.15-393.15	4.13-8.76	4-440	0.57-722.6	This work
Model (N_2/heptane)	0.34-41.7	313.15-393.15	8.33-15.34	0-100	19-23.32	This work
Model (N_2/hexadecane)	0.34-41.7	313.15-393.15	1.82-7.23	0-95.5	0-35.2	This work
Model (N_2/oil)	20	333.15	5.55×10^{-3}			[45]
Model (CO_2/heavy oil)	5.52	323.15	226.8	2.02		[46]
Experiment (CO_2/heptane)	7.31	313.15	5.92			[47]
Experiment (CO_2/hexadecane)	5.28	298.15	2.64			[48]
Experiment (CO_2/hexadecane)	3.46	323.15	3.47			[37]
Model (CO_2/Ontario oil)	2.9	298.15	1.14	5.7		[28]
Model (CO_2/Weyburn oil)	0.1-5	300.15	0.47-2.49	0.88-8.41	2.3-6.8	[1]
Model (CO_2/heavy oil)	3.51	294.15	16.5		<0.6	[20]

an easier diffusion process. Interfacial resistance in N_2/hexadecane system decreases at higher pressure, because gas solubility is improved as pressure increases. Larger amounts of gas dissolved in the liquid phase result in more liquid viscosity reduction. On the other hand, at higher pressures there is a lower resistance in interface for gas molecules to pass through it (interfacial resistance graph versus pressure for N_2/hexadecane system is shown in Fig. S2 of the Supplementary data) [1,2].

Fig. 7 shows changes of interfacial resistance (1/k) versus temperature for N_2/heptane system. In Fig. 7 a similar trend is observed and interfacial resistance reduces as temperature and pressure increase (interfacial resistance graph versus pressure for N_2/heptane system is shown in Fig. S3 of the Supplementary data).

In general, interfacial resistance in N_2/hexadecane system is higher than in N_2/heptane system; because heptane has lower viscosity than hexadecane, diffusion of N_2 can occur easier than hexadecane.

Two phenomena, diffusivity and solubility, determine the behavior of interface mass transfer coefficient with temperature. Increasing temperature from one side enhances diffusion process rate; on the other side it reduces the solubility of gas in liquid phase. Positive effect of temperature on interface mass transfer coefficient implies that in these systems, the diffusion phenomenon controls the mass transfer process; it was found that the interfacial resistance decreases as the temperature increases. Meanwhile, at lower pressure, the slope of the interfacial resistance curves versus temperature is higher, hence, it can be said that at lower pressures increasing temperature has remarkable effect on reduction of interfacial resistance.

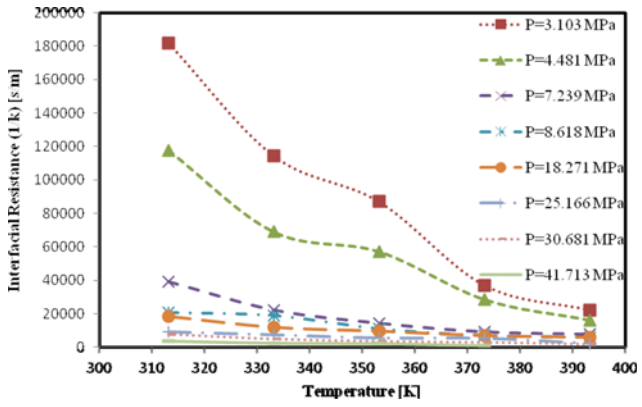

Fig. 6. Interfacial resistance changes with temperature for N_2/hexadecane system.

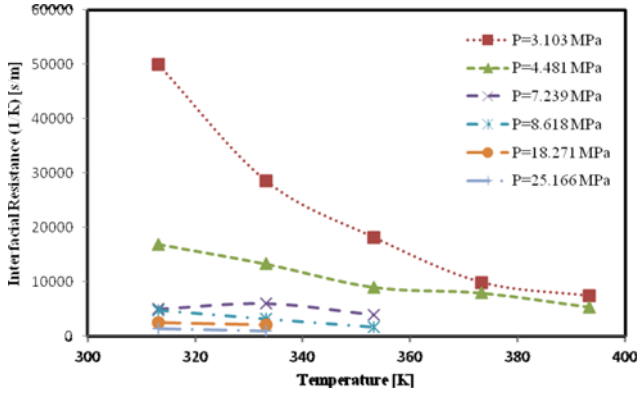

Fig. 7. Interfacial resistance changes with temperature for N_2/heptane system.

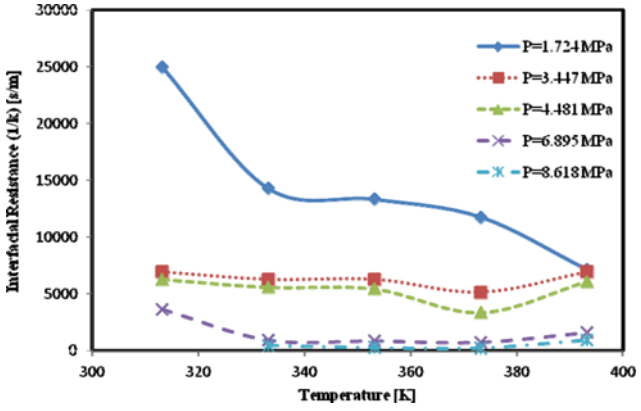

Fig. 8. Interfacial resistance changes with temperature for CO_2/hexadecane system.

4. Comparison of Interface Mass Transfer Coefficient in N_2/Alkane and CO_2/Alkane Systems

Fig. 8 below shows interfacial resistance as a function of temperature for CO_2/hexadecane system.

According to Fig. 8, interfacial resistance reduces monotonically at low pressures. As the temperature increases, for CO_2/hexadecane system, at moderate pressures (from 3.447 to 8.618 MPa), the interfacial resistance decreases by increasing temperature at the first step and then increases. In this case, as for N_2/hexadecane and N_2/heptane systems, the interactions of diffusion and solubility ultimately determine the behavior of the system by raising temperature. The temperature increase from one hand improves gas diffusion process and decreases interfacial resistance; on the other hand, it reduces solubility of gas in the liquid phase and increases interfacial resistance. In other words, at lower temperatures, with reduction of interfacial resistance, diffusion controls the process, while at higher temperatures solubility dominates and interfacial resistance almost remains constant as the temperature increases. In this system, like N_2/liquid hydrocarbon systems, increasing pressure improves mass transfer process and interfacial resistance reduces (Interfacial resistance graph versus pressure for CO_2/hexadecane system has been shown in Fig. S4 of the Supplementary data).

In Fig. 9, interfacial resistance behavior of CO_2/heptane system is illustrated as a function of temperature.

Similar trends are observed in Figs. 8 and 9, for CO_2/hexadecane and CO_2/heptane systems. For CO_2/heptane system, at low to moderate pressures (from 3.45 to 4.48 MPa), interfacial resistance decreases first and then increases. It means that, in this case, as for CO_2/hexadecane system, diffusion takes over the negative solubility effects and increasing temperature causes interfacial resistance to reduce. However, solubility becomes important and controls the interfacial resistance behavior at higher temperatures. Interfacial resistance in CO_2/hexadecane systems is generally higher than in CO_2/heptane which is due to higher viscosity of hexadecane relative to heptane (interfacial resistance curve as a function of pressure for CO_2/heptane system has been shown in Fig. S5 of Supplementary data).

By comparison of Figs. 6 to 9, it is concluded that in the systems which contained N_2 as the gas phase, interfacial resistance is generally higher than in CO_2/alkane systems, because miscibility pressure of N_2/alkane mixtures is significantly higher than CO_2/alkanes. However, in systems in which heptane is employed as the liquid phase, interfacial resistance has less value than those which contain hexadecane. This issue can be attributed to the fact that lower viscosity of heptane compared to hexadecane makes it easier for gas molecules to diffuse. However, in N_2/liquid hydrocarbon mixtures, at all studied temperatures and pressures, increasing the temperature decreases the interfacial resistance; therefore, for all temperatures and pressures studied in this paper for N_2/hexadecane and N_2/heptane systems, the diffusion mechanism is the governing mass transfer mechanism.

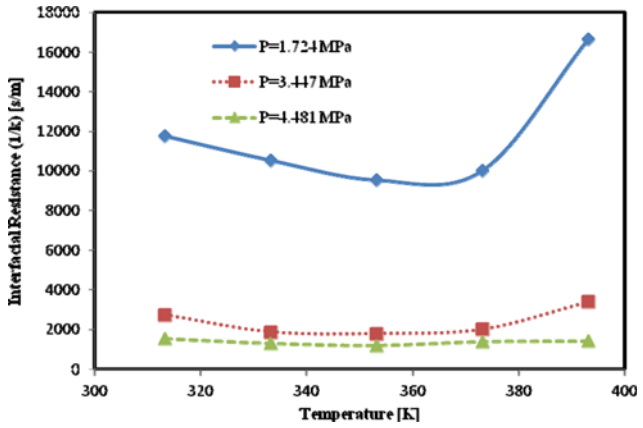

Fig. 9. Interfacial resistance changes with temperature for CO_2/heptane system.

5. Application of the Results in Petroleum Industry

Gas injection is considered as one of the most promising methods among the enhanced oil recovery (EOR) techniques [49-51]. Molecular diffusion plays an important role in chemical and petroleum engineering and is described as the predominant mass transfer mechanism in miscible or immiscible gas injection processes [20,22]. In particular, accurate estimation of interfacial resistance and diffusion parameters is of great importance for designing and improving gas injection techniques for enhanced oil recovery. According to the results of this study, N_2 injection improves by increasing pressure and temperature; therefore, it can be considered as an effective EOR technique for hydrocarbon reservoirs at high pressure and temperature. However, interfacial resistance estimation shows that CO_2 injection is regarded as appropriate at optimized temperature and high pressure conditions. Meanwhile, because of higher interfacial resistance of N_2/ alkane systems, N_2 injection is more suitable for light hydrocarbon reservoirs, while CO_2 injection can be used to enhance oil recovery in light to medium hydrocarbon reservoirs.

CONCLUSIONS

Interfacial resistance was examined to confirm the importance of this resistance during th mass transfer process. For estimating the interfacial resistance, interfacial mass transfer coefficients were evaluated as a function of pressure and temperature. The gas-oil systems used here consist of N_2/hexadecane and N_2/heptane systems, and the obtained results were compared with those of CO_2/hexadecane and CO_2/heptane systems. Experiments were carried out at different temperatures and pressures to measure dynamic and equilibrium IFT data for gas-liquid systems. IFT experiments were carried out utilizing pendant drop method at high pressures and temperatures. The mass transfer process was modeled and the mass transfer coefficients were evaluated at five different temperatures (from 313.15 to 393.15 K with an interval of twenty-fold) and pressure range of 0.34 to 41.7 MPa.

Results showed that interfacial resistance in the systems in which N_2 acts as gas phase is greater than in CO_2 systems. Moreover, systems with lighter paraffinic liquid phase have lower interfacial resistance.

For N_2/hexadecane and N_2/heptane systems, in all studied ranges of pressure and temperature, interfacial resistance decreases as the temperature and pressure increase, and this issue demonstrates diffusion dominates the solubility. In contrast, in CO_2/hexadecane

and CO_2/heptane, the interfacial resistance is reduced initially as the temperature increases and then it starts to increase in most cases. Hence, it is concluded that, in the first stage, the diffusion mechanism controls the process and then solubility governs the gas liquid mass transfer process. However, in both CO_2/alkane and N_2/alkane systems the interfacial resistance declines as the pressure increase for the whole study. These results could be extended to the systems of non-hydrocarbon gas and crude oil systems for enhancing oil recovery.

ACKNOWLEDGEMENTS

The authors are thankful to the research council of the Shiraz University for financial supports and providing the laboratory and the computational facilities required by the research. Financial supports from Enhanced Oil Recovery (EOR) Center of the College of Engineering are acknowledged.

NOMENCLATURE

r_n : inner radius of needle [m]
t : time [s]
B_{im} : boundaries between liquid and impermeable surfaces
B_{int} : boundaries between liquid and gas
c : gas concentration in liquid phase [mol/m^3]
D : diffusion coefficient [m^2/s]
n_r : direction cosine
n_z : direction cosine
k : interface mass transfer coefficient [m/s]
C_{eq} : equilibrium concentration of gas in liquid [mol/m^3]
C : dimensionless gas concentration
R : radial coordinate
Z : axial coordinate
k_D : mass transfer Biot number
E : objective function
IFT_{exp} : experimental interfacial tension [mN/m]
IFT_{cal} : estimated interfacial tension [mN/m]

Greek Letters

φ : physical domain
τ : dimensionless time
θ : computational domain

REFERENCES

1. D. Yang and Y. Gu, *Ind. Eng. Chem. Res.*, **47**, 5447 (2008).
2. D. Yang and Y. Gu, SPE102481 the SPE Annual Technical Conference and Exhibition, San Antonio, Texas, U.S.A. (2006).
3. D. Yang, P. Tontiwachwuthikul and Y. Gu, *J. Chem. Eng. Data*, **50**, 1242 (2005).
4. D. Yang and Y. Gu, *Pet. Sci. Technol.*, **23**, 1099 (2005).
5. I. S. Khattab, F. Bandarkar, M. A. A. Fakhree and A. Jouyban, *Korean J. Chem. Eng.*, **29**, 812 (2012).
6. S. C. Ayirala and D. N. Rao, *J. Colloid Interface Sci.*, **299**, 321 (2006).
7. S. C. Ayirala and D. N. Rao, *Fluid Phase Equilib.*, **249**, 82 (2006).
8. W. Lewis and W. Whitman, *Ind. Eng. Chem.*, **16**, 1215 (1924).
9. L. Scriven and R. Pigford, *AIChE J.*, **4**, 439 (1958).
10. L. Scriven and R. Pigford, *AIChE J.*, **5**, 397 (1959).
11. R. Searle and K. F. Gordon, *AIChE J.*, **3**, 490 (1957).
12. J. A. Rhim and J. H. Yoon, *Korean J. Chem. Eng.,* **22**, 201 (2005).
13. R. W. Schrage, *A theoretical study of interphase mass transfer*, Columbia University Press (1953).
14. R. E. Treybal, *Mass-transfer operations*, McGraw-Hill, New York (1980).
15. H.-C. Yang, J.-H. Kim, Y.-C. Seo and Y. Kang, *Korean J. Chem. Eng.*, **13**, 261 (1996).
16. R. De Boer, S. Wellington and K. Tschiedel, *Colloids Surf.*, **9**, 79 (1984).
17. H. Reamer, J. Opfell and B. Sage, *Ind. Eng. Chem.*, **48**, 275 (1956).
18. S. M. Walas, *Modeling with differential equations in chemical engineering*, Butterworth-Heinemann Boston, MA (1991).
19. F. Civan and M. Rasmussen, *SPE J.*, **11**, 71 (2006).
20. A. K. Tharanivasan, C. Yang and Y. Gu, *J. Pet. Sci. Eng.*, **44**, 269 (2004).
21. H. Saboorian Jooybari, SPE 157734 the SPE Heavy Oil Conference, Calgary, Alberta, Canada (2012).
22. S. R. Etminan, M. Pooladi-Darvish, B. Maini and Z. J. Chen, CSUG/SPE 138191 the Canadian Unconventional Resources and International Petroleum Conference, Calgary, Alberta, Canada (2010).
23. N. Policarpo, SPE 160912-STU the SPE Annual Technical Conference and Exhibition, San Antonio, Texas, U.S.A. (2012).
24. F. Civan and M. L. Rasmussen, SPE 75135 the SPE/DOE Improved Oil Recovery Symposium, Tulsa, OK (2002).
25. F. Civan and M. L. Rasmussen, SPE 67319 the SPE Mid Continent Operations Symposium, Oklahoma City, OK (2001).
26. Y. Zhang, C. Hyndman and B. Maini, *J. Pet. Sci. Eng.*, **25**, 37 (2000).
27. C. Yang and Y. Gu, *Ind. Eng. Chem. Res.*, **44**, 4474 (2005).
28. Y. Chaodong and G. Yongan, SPE 84202 the SPE Annual Technical Conference and Exhibition, Denever, Colorado, U.S.A. (2003).
29. J. Drelich, C. Fang and C. White, *Encyclopedia of Surface and Colloid Science*, 3152 (2002).
30. J. Jůza, *Czech. J. Phys*., **47**, 351 (1997).
31. A. Zolghadr, M. Escrochi and S. Ayatollahi, *J. Chem. Eng. Data*, **58**, 1168 (2013).
32. A. Zolghadr, M. Riazi, M. Escrochi and S. Ayatollahi, *Ind. Eng. Chem. Res.*, **52**, 9851 (2013).
33. D. Yang, *Interfacial interactions of the crude oil-reservoir brine-reservoir rock systems with dissolution of carbon dioxide under reservoir conditions*, Ph.D. Dissertation, University of Regina, Canada (2005).
34. R. Ghez, *Diffusion phenomena: Cases and studies*, Springer (2001).
35. F. Civan and M. Rasmussen, SPE 84072 the SPE Annual Technical Conference and Exhibition, Denver, Colorado, U.S.A. (2003).
36. E. Saatdjian and W. Janna, *Appl. Mech. Rev.*, **54**, 72 (2001).
37. M. A. Matthews, J. B. Rodden and A. Akgerman, *J. Chem. Eng. Data*, **32**, 319 (1987).
38. R. H. Perry, D. W. Green and J. O. Maloney, *Perry's chemical engineers' handbook*, McGraw-Hill, New York (2008).
39. Y. Gu and D. Yang, Paper 2004-083 the 55th Canadian International Petroleum Conference, Calgary, Alberta, Canada (2004).
40. M. Nobakht, S. Moghadam and Y. Gu, *Fluid Phase Equilib.*, **265**, 94 (2008).
41. M. Nobakht, S. Moghadam and Y. Gu, *Ind. Eng. Chem. Res.*, **47**,

8918 (2008).
42. B. Kvamme, T. Kuznetsova, A. Hebach, A. Oberhof and E. Lunde, *Compu. Mater. Sci.*, **38**, 506 (2007).
43. T. Nguyen and S. Farouq Ali, *J. Can. Pet. Technol.*, **37**, 24 (1998).
44. R. Simon and D. Graue, *J. Pet. Technol.*, **17**, 102 (1965).
45. P. Guo, Z. Wang, Y. Xu and J. Du, *Mass Transfer in Chemical Engineering Processes*, November 4 (2011), DOI:10.5772/22868.
46. E. Zamanian, M. Hemmati and M. S. Beiranvand, *Nafta*, **63**, 351 (2012).
47. H. Saad and E. Gulari, *J. Phys. Chem.*, **88**, 136 (1984).
48. A. Grogan, V. Pinczewski, G. Ruskauff and O. FM, *SPE Reservoir Eng.*, **3**, 93 (1988).
49. G. Moritis, *Oil Gas J.*,**102**, 45 (2004).
50. F. Stalkup Jr., *Miscible Displacement,* Monograph Series, SPE Richardson, TX (1983).
51. S. Ali and S. Thomas, *J. Can. Pet. Technol.*, **39**, 7 (2000).